All these results could be extended to statically indeterminate structures but with a more delicate physical interpretation. In practice, effective mass models are only currently used for rigid junctions.

5.4. Modal effective parameters and dynamic responses

5.4.1. *Frequency responses*

Relations [5.35] to [5.37] show that any FRF $X(\omega)$ coming from $\mathbf{G}_{ii}(\omega)$, $\mathbf{T}_{ij}(\omega)$ or $\mathbf{M}_{jj}(\omega)$ is of the form:

$$X(\omega) = \sum_{\underline{k}} A_{\underline{k}}(\omega)\, \widetilde{X}_{\underline{k}} + X_{res} \qquad [5.57]$$

(subscripts of the DOF omitted for the sake of convenience, excluding the statically indeterminate term from [5.37]) with:

– $A_{\underline{k}}(\omega)$ dynamic amplification $H_{\underline{k}}(\omega)$ or $T_{\underline{k}}(\omega)$;

– $\widetilde{X}_{\underline{k}}$ modal effective parameter $\widetilde{G}_{\underline{k}}$, $\widetilde{T}_{\underline{k}}$ or $\widetilde{M}_{\underline{k}}$;

– X_{res} residual parameter G_{res}, T_{res} or M_{res}.

Other types of FRF are deduced by multiplying or dividing by $i\omega$. Form [5.57] is therefore general. Graphically, its amplitude using logarithmic scales is illustrated schematically in Figure 5.7. The profile is governed by the following rules:

– at a very low frequency, we converge towards the static value equal to the sum of the effective parameters of the retained modes, increased by the residual parameter representing the truncated modes and possibly the junction itself (relations [5.38] to [5.40]). Exceptions are the flexibilities of structures with rigid-body modes and the masses of statically indeterminate structures which have a contribution in $1/\omega^2$;

– when the frequency increases, each mode creates a peak corresponding to its resonance which is predominant if it is relatively isolated and if its effective parameter is not too small. Otherwise, it can combine with the neighboring modes and perhaps disappear visually from the curve;

– between two peaks, i.e. a minimum occurs between two consecutive modes which are not too close and with similar importance. This minimum will take one of the following two forms according to the corresponding phases:

- if the effective parameters of the two modes are of the same sign, the two contributions are antagonist and result in a very small amplitude, hence an “anti-peak” corresponding to an anti-resonance, the sharpness of which is similar to that of the neighboring peaks. For a sine motion at this frequency, this is a vibrational node. With reference to the last comment in section 5.2.1, any driving-point FRF should present only anti-resonances,

- if the effective parameters of the two modes are of an opposite sign, the two contributions add to each other and give a significant amplitude, hence a local minimum or “trough”. There shouldn't be any in a driving-point FRF. Conversely, a transfer FRF may have both anti-resonances and local minima depending on the signs of the corresponding effective parameters.

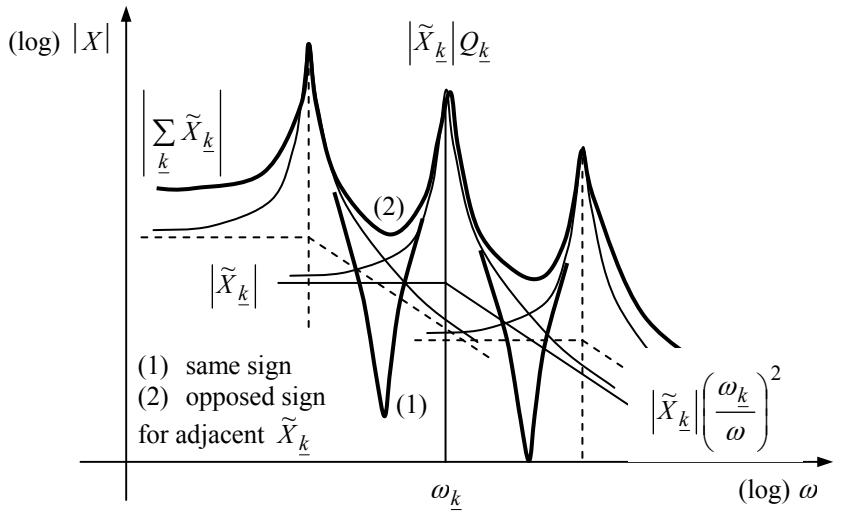

Figure 5.7. *FRF profile $G(\omega)$, $T(\omega)$ or $M(\omega)$*

The FRF profile can vary considerably according to the value of the effective parameters, damping and the proximity of the modes. Generally, the peaks are rather well distinguished at low frequencies where the modal density is low, then become progressively coupled towards the high frequencies. In an experimental context, measurement noise may perturb the profile to a certain degree and mask certain aspects, especially the anti-resonances.

Note that for a given structure, the peaks of all FRF will be located at the same frequencies, those of the normal modes, while the frequencies of the anti-resonances will depend on the FRF considered.

As an illustration several different possible situations with the simple cases in Figures 4.1 and 4.3, we obtain the following plots:

– Figures 5.8 relative to the 2 internal DOF system of Figure 4.1 and to the results of [4.9] and [5.11]:

- Figure 5.8a: $G_{11}(\omega) = (3/5k)\, H_1(\omega) + (2/5k)\, H_2(\omega)$

- Figure 5.8b: $G_{12}(\omega) = (6/5k)\, H_1(\omega) + (-1/5k)\, H_2(\omega)$

- Figure 5.8c: $G_{22}(\omega) = (12/5k)\, H_1(\omega) + (1/10k)\, H_2(\omega)$

- Figure 5.8d: $T_{10}(\omega) = (3/5)\, T_1(\omega) + (2/5)\, T_2(\omega)$

- Figure 5.8e: $T_{20}(\omega) = (6/5)\, T_1(\omega) + (-1/5)\, T_2(\omega)$

- Figure 5.8f: $M_{00}(\omega) = (9m/5)\, T_1(\omega) + (m/5)\, T_2(\omega)$

– Figure 5.9 relative to the 3-DOF free system in Figure 4.3 and to the results of [4.16] and [5.12]:

- Figure 5.9a: $G_{11}(\omega) = -1/(3m\omega^2) + (1/2k)\, H_2(\omega) + (1/18k)\, H_3(\omega)$

- Figure 5.9b: $G_{13}(\omega) = -1/(3m\omega^2) + (-1/2k)\, H_2(\omega) + (1/18k)\, H_3(\omega)$

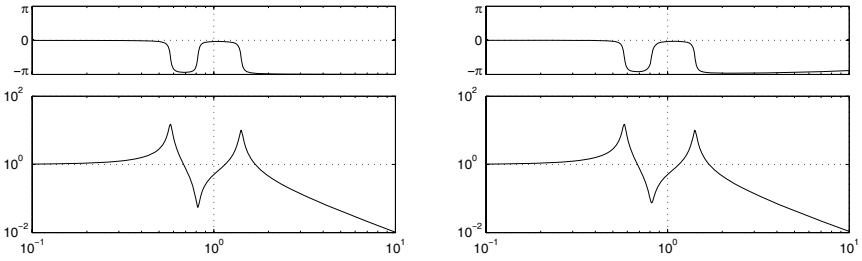

a) $G_{11}(\omega)$ d) $T_{10}(\omega)$

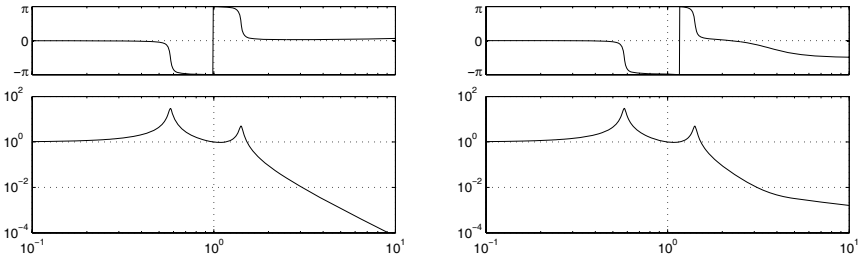

b) $G_{12}(\omega)$ e) $T_{20}(\omega)$

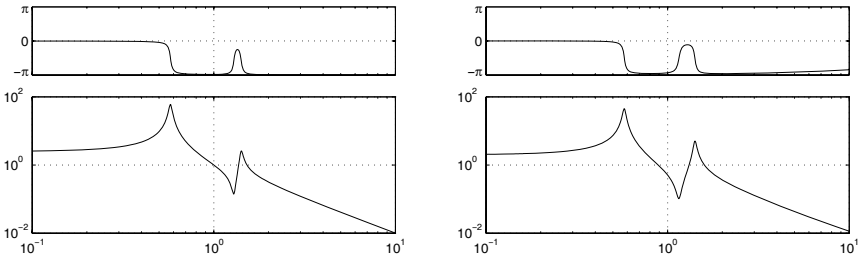

c) $G_{22}(\omega)$ d) $M_{00}(\omega)$

Figure 5.8. *FRF for the 2 internal DOF system in Figure 4.1*
($m = k = 1$, $\zeta_k = 2\% \Leftrightarrow Q_k = 25$)

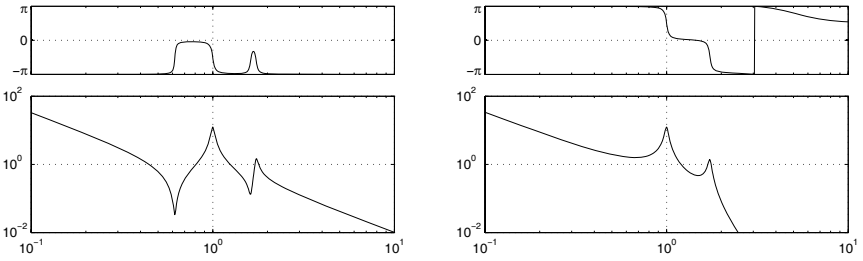

a) $G_{11}(\omega)$ b) $G_{13}(\omega)$

Figure 5.9. *FRF for the 3-DOF free system in Figure 4.3*
($m = k = 1$, $\zeta_k = 2\% \Leftrightarrow Q_k = 25$)

5.4.2. *Random responses*

In the case of a random excitation x defined by its PSD $S_{xx}(\omega)$ (see section 1.2.3.4), the response y defined by its PSD $S_{yy}(\omega)$ is deduced from this using equation [1.39]. Starting from relation [5.57], we can thus write:

$$S_{yy}(\omega) = \left| \sum_{\underline{k}} A_{\underline{k}}(\omega)\, \widetilde{X}_{yx,\underline{k}} + X_{yx,res} \right|^2 S_{xx}(\omega) \qquad [5.58]$$

The case of the 1-DOF was already discussed in section 2.2.5 in order to obtain the response PSD and the rms values. Since each mode behaves like a 1-DOF system, it is easy to deduce the following results for the rms values of the responses.

With the following hypotheses:

– the excitation PSD $S_{xx}(\omega)$, renamed $W_x(f)$ as in section 2.2.5 for the practical applications, varies slowly in the vicinity of each natural frequency, so that the value $W_x(f_{\underline{k}})$ is used for the contribution of each mode $\underline{k}$;

– the natural frequencies $f_{\underline{k}}$ are well separated, so that it is possible to replace the integral of the sum with the sum of the integrals, as illustrated in Figure 5.10; then, the mean squares are given by the relation:

$$\overline{y^2} \approx \sum_{\underline{k}} \left(\frac{\pi}{2} f_{\underline{k}}\, Q_{\underline{k}} \right) \widetilde{X}^2_{yx,\underline{k}}\, W_x(f_{\underline{k}}) + X^2_{yx,res}\, \overline{x^2} \qquad [5.59]$$

Each mode contributes to the mean square by the product of the term $(\pi/2) f_{\underline{k}}\, Q_{\underline{k}}$, resulting from the integration of its dynamic amplification, with the square of the implied effective parameter and the excitation PSD at its natural frequency. As for the residual term, its contribution is the product of its square by the excitation mean square. Relation [5.59] is easy to interpret more particularly in the light of the scheme in Figure 5.2a.

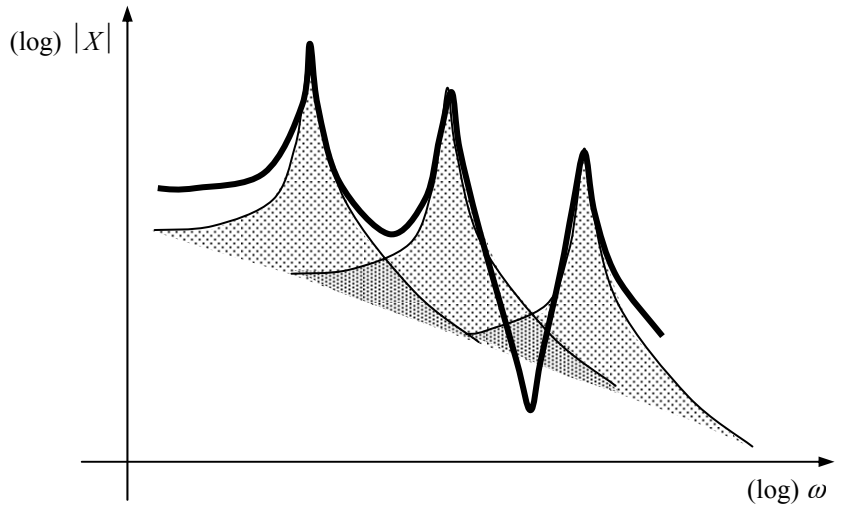

Figure 5.10. *Integration of the response PSD in order to find the rms values*

The preceding results are valid only for one excitation and one response. They may be extrapolated to several excitations and responses based on expression [1.42] replacing [1.39].

With the example of the 2 internal DOF system in Figure 4.1 subjected to a white noise in acceleration $W_{\ddot{u}0}$ at its base, the mean square of the response on DOF 2 is given by (with $Q_{\underline{k}} = 10$ and the results [4.9] and [5.11]) :

$$\overline{\ddot{u}_2{}^2} \approx \frac{\pi}{2}\frac{10}{2\pi}\sqrt{\frac{k}{m}}\, W_{\ddot{u}0}\left(\left(\frac{6}{5}\right)^2\sqrt{\frac{1}{3}}+\left(-\frac{1}{5}\right)^2\sqrt{2}\right) \approx (2.08+0.14)\sqrt{\frac{k}{m}}\, W_{\ddot{u}0} \quad [5.60]$$

5.4.3. *Time responses*

For a FRF $X(\omega)$ of form [5.57], the response $y(t)$ to an excitation $x(t)$ is given by the convolution integral [1.30] with the unit impulse response given by the inverse Fourier transform FT^{-1} of $X(\omega)$. By writing that the transform of the sum is equal to the sum of the transforms, we obtain:

$$y(t) = \sum_{\underline{k}} \left(\int_{-\infty}^{t} x(\tau)\, \mathrm{FT}^{-1}\left(A_{\underline{k}}(\omega) \right) \mathrm{d}\tau \right) \tilde{X}_{yx,\underline{k}} + y_{res}(t) \qquad [5.61]$$

we can see that each mode contributes to the response by a product, that of the effective parameter with the convolution of the excitation and the unit impulse response $h_{\underline{k}}(t)$ or $t_{\underline{k}}(t)$ of relations [2.60] or [2.61]. With regard to the residual term, it provides a residual term for the response in a similar way.

Using the example of the 2 internal DOF in Figure 4.1 subjected to an acceleration impulse at its base, the time responses in Figure 5.11 are obtained:

– Figure 5.11a: response on DOF 1: $\ddot{u}_1(t) = (3/5)\, t_1(t) + (2/5)\, t_2(t)$;

– Figure 5.11b: response on DOF 2: $\ddot{u}_2(t) = (6/5)\, t_1(t) + (-1/5)\, t_2(t)$.

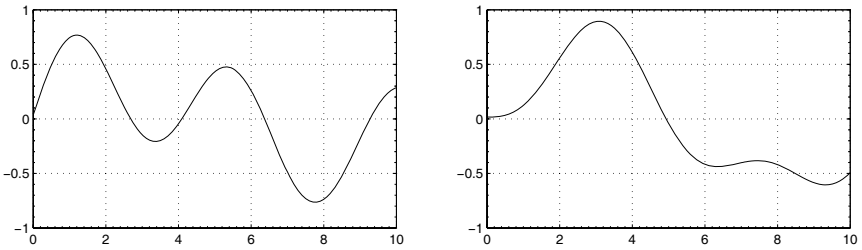

Figure 5.11. *Impulse response of the 2 internal DOF system in Figure 4.1* ($m = k = 1$, $\zeta_k = 2\% \Leftrightarrow Q_k = 25$)

5.4.4. *Time response extrema*

The response spectra introduced in section 2.3.3 provide the response extrema of a 1-DOF system subjected to the excitation considered. Since each mode behaves

like a 1-DOF system, the information about the response extrema of the structure can be deduced. For example, with an absolute acceleration spectrum $S_{\ddot{u}}(f)$ of a transient applied to the base of a structure, the use of an effective mass model as illustrated by Figure 5.2 makes it possible to easily establish the following results:

– the spectrum gives by definition the maximum acceleration of each effective mass;

– by multiplying the maximum acceleration by the effective mass, we obtain the maximum reaction at the base due to each mode;

– by multiplying the maximum acceleration by the effective transmissibility between the base and an internal DOF *i* (relation [5.55]), we obtain the maximum acceleration on this DOF due to each mode.

Therefore, this gives us the maximum contributions of each mode. If we now want to obtain the maximum responses of the structure, it is necessary to combine these results. As the maxima of the different modes do not generally have any reason to occur at the same time, the exact recombination is not possible. This is the consequence of the loss of information in the spectrum which retains only the amplitude (last note in section 2.3.3). The modal maxima can only be combined approximately, for example:

– by a direct sum, which will necessarily give an overestimation of the levels although this is a conservative approach, it can be very pessimistic;

– by a quadratic sum, which will probably be closer to reality, but can also underestimate the levels;

– by a mixed sum, i.e. direct for certain terms and quadratic for other terms, for example the highest maximum combined with the square root of the quadratic sum of the others. The quality of the result will depend on the case considered.

With the example of the 2 internal DOF in Figure 4.1 subjected to an acceleration impulse at its base, the results on DOF 1 and 2 with a modal viscous damping of 5% ($Q = 10$) are the following:

– exact results given in section 5.4.3:

$$\frac{|\ddot{u}_1|_{\max}}{\sqrt{k/m}} \approx 0.7480 \quad \frac{|\ddot{u}_2|_{\max}}{\sqrt{k/m}} \approx 0.8281$$

– direct sum:

$$\frac{|\ddot{u}_1|_{\max}}{\sqrt{k/m}} \approx 0.3226 + 0.5268 = 0.8495 \quad \frac{|\ddot{u}_2|_{\max}}{\sqrt{k/m}} \approx 0.6453 + 0.2634 = 0.9087$$

– quadratic sum:

$$\frac{|\ddot{u}_1|_{\max}}{\sqrt{k/m}} \approx 0.6178 \quad \frac{|\ddot{u}_2|_{\max}}{\sqrt{k/m}} \approx 0.6970$$

In this particular case, the quadratic sum clearly underestimates the levels. With a larger number of modes, a judicious combination of sums can provide an acceptable approximation.

5.5. Industrial examples

As an illustration of the modal effective parameters in an industrial context, a first example is given with the model in Figure 5.12, which represents a marine support structure.

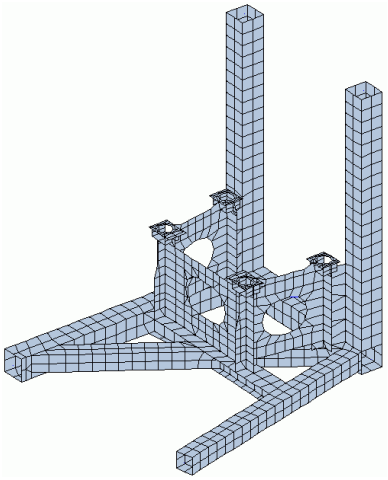

Figure 5.12. *Marine support structure (with the permission of CTSN Toulon)*

We are interested in the transmissibility of the vibrations between the motor interface (average of 4 attachment points using a single node) and the support (rigid junction using a single node).

The effective modal transmissibilities between two DOF in the same direction for the first 43 modes (up to 500 Hz) are given by Table 5.3 and plotted in Figure 5.13a, in a presentation that can be generalized to any type of effective parameter. For each mode k, of frequency f_k, this table provides the value of the effective

parameter and the cumulative sum, in absolute and relative values with respect to the corresponding static term, here 1. The term makes it possible to appreciate the importance of each mode in relation to the considered FRF, the sum makes it possible to verify the convergence toward the static term. The FRF is not a driving-point FRF here and can have positive or negative effective parameters, hence a non-monotone convergence, contrary to what a driving-point FRF would give. The first 5 transmissibilities are positive and quite large: 20% of the static for the first one, 59% for the second, etc. The sixth one is negative, the seventh one is positive again, etc. They can clearly be seen again in Figure 5.13a where each jump of the sum shows the term with its sign.

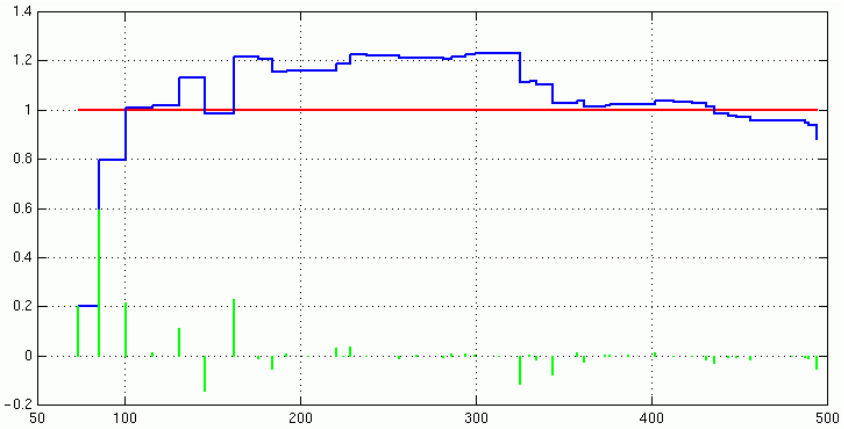

a) Effective transmissibilities

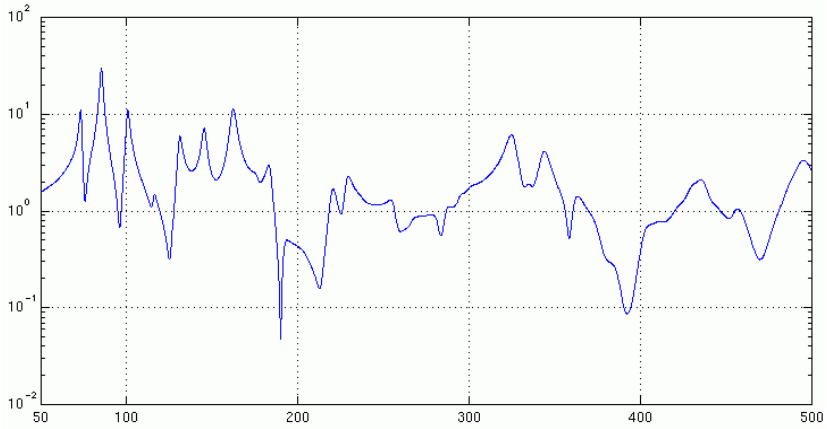

b) Dynamic transmissibility

Figure 5.13. *Effective transmissibilities and dynamic transmissibility along Y of the model in Figure 5.12*

k	fk (Hz)	Effective parameter Term	Effective parameter Sum	effective/static parameter Term	effective/static parameter Sum
1	73.21	2.02640e-01	2.02640e-01	0.20264	0.20264
2	85.16	5.91011e-01	7.93650e-01	0.59101	0.79365
3	100.57	2.13382e-01	1.00703e+00	0.21338	1.00703
4	115.49	1.18260e-02	1.01886e+00	0.01183	1.01886
5	130.77	1.12945e-01	1.13180e+00	0.11294	1.13180
6	145.24	-1.45066e-01	9.86737e-01	-0.14507	0.98674
7	162.14	2.29125e-01	1.21586e+00	0.22913	1.21586
8	176.12	-9.94615e-03	1.20592e+00	-0.00995	1.20592
9	183.61	-5.35969e-02	1.15232e+00	-0.05360	1.15232
10	191.52	7.24342e-03	1.15956e+00	0.00724	1.15956
11	204.39	-3.83887e-04	1.15918e+00	-0.00038	1.15918
12	220.17	3.05485e-02	1.18973e+00	0.03055	1.18973
13	224.20	-1.45466e-05	1.18971e+00	-0.00001	1.18971
14	228.43	3.41062e-02	1.22382e+00	0.03411	1.22382
15	237.66	-1.45901e-03	1.22236e+00	-0.00146	1.22236
16	256.00	-1.29035e-02	1.20946e+00	-0.01290	1.20946
17	266.28	2.48120e-03	1.21194e+00	0.00248	1.21194
18	281.37	-6.03675e-03	1.20590e+00	-0.00604	1.20590
19	285.96	9.87278e-03	1.21577e+00	0.00987	1.21577
20	293.66	8.08338e-03	1.22386e+00	0.00808	1.22386
21	299.20	4.90771e-03	1.22876e+00	0.00491	1.22876
22	313.17	-7.04854e-04	1.22806e+00	-0.00070	1.22806
23	325.21	-1.14711e-01	1.11335e+00	-0.11471	1.11335
24	330.40	4.22691e-03	1.11758e+00	0.00423	1.11758
25	334.56	-1.68215e-02	1.10075e+00	-0.01682	1.10075
26	343.32	-7.51423e-02	1.02561e+00	-0.07514	1.02561
27	357.37	1.17607e-02	1.03737e+00	0.01176	1.03737
28	361.63	-2.34121e-02	1.01396e+00	-0.02341	1.01396
29	373.38	2.91438e-03	1.01687e+00	0.00291	1.01687
30	375.93	3.79900e-03	1.02067e+00	0.00380	1.02067
31	386.76	2.89954e-03	1.02357e+00	0.00290	1.02357
32	401.78	1.16100e-02	1.03518e+00	0.01161	1.03518
33	412.54	-2.89955e-03	1.03228e+00	-0.00290	1.03228
34	423.13	-3.77455e-03	1.02851e+00	-0.00377	1.02851
35	430.96	-1.48424e-02	1.01367e+00	-0.01484	1.01367
36	435.83	-3.07169e-02	9.82950e-01	-0.03072	0.98295
37	443.61	-8.05702e-03	9.74893e-01	-0.00806	0.97489
38	448.63	-4.36527e-03	9.70527e-01	-0.00437	0.97053
39	456.26	-1.42071e-02	9.56320e-01	-0.01421	0.95632
40	480.29	-2.04802e-03	9.54272e-01	-0.00205	0.95427
41	487.30	-8.61732e-03	9.45655e-01	-0.00862	0.94565
42	489.43	-9.06207e-03	9.36593e-01	-0.00906	0.93659
43	494.36	-5.55478e-02	8.81045e-01	-0.05555	0.88104
			---		---
	Sum	:	8.81045e-01		0.88104
	Static term	:	1.00000e+00		1.00000
	Residual term	:	1.18955e-01		0.11896

Table 5.3. *Effective transmissibilities along Y of the model in Figure 5.12*

Figure 5.13b illustrates, with the same frequency scale, the dynamic transmissibility amplitude for a global structural damping of 0.02 (amplification of 50 at resonances for all modes). This parallel clearly illustrates the considerations in section 5.4.1. At a very low frequency, the response converges towards the static value of 1. Then, when the frequency increases, each mode creates a peak, which corresponds to its resonance where it is predominant if it is relatively isolated and if its effective parameter is not too small, which is the case for the first modes. Some anti-resonances or some local maxima are found between the peaks according to the signs of the effective parameters, starting with anti-resonances followed by the appearance of local minima. At higher frequencies, the variations become harder to distinguish.

We will take the model in Figure 3.11 with its 19 modes below 150 Hz so as to illustrate the analysis possibilities of a model according to its effective masses with regard to its rigid junction. Table 5.4 presents the diagonal terms of the 6×6 effective mass matrix for each mode. Note that they provide nearly all the necessary information, according to relation [5.47], allowing us to determine the participation factors except for their sign. This table gives the following information, for example:

– the first mode is a global lateral mode in direction *Y* with a directional mass of 92.8 kg, having more than a quarter of the total mass and an inertia of 41.4 m^2.kg, hence a center of mass at $(41.4/92.8)^{1/2} = 0.668$ m along *Z*. Therefore, it is a global lateral model along *Y*, with a small component in torsion around *X* and a very small lateral component along *Z*;

– the second mode is also lateral in direction *Y* with a smaller directional mass but a significantly higher center of mass along *Z*. The third mode is lateral in the direction *Z* with more than half of the total mass. The fourth mode is an axial mode, the fifth one is relatively secondary, etc.;

– the first 19 modes represent about 88% of the mass along *Y* and *Z*, but only 48% of the mass along *X*, hence a more important residual term along *X*.

These properties make it possible to clearly understand the importance of each mode in relation to the rigid junction and to predict the form of the dynamic mass of the model, seen from its base, just like the dynamic transmissibility of the preceding example.

We can deduce the effective mass model according to the considerations of section 5.3.2. We arrive at the ingredients of Table 5.5 and at the illustration of Figure 5.14.

k	fk	Mx	My	Mz	Ix	Iy	Iz
1	41.36	0.000	92.797	0.004	5.426	0.006	41.380
2	45.88	0.001	47.891	0.007	1.267	0.019	192.044
3	52.16	1.920	0.000	181.962	0.001	262.336	0.003
4	82.19	103.594	0.006	0.010	0.000	0.578	0.001
5	87.25	7.009	0.008	0.222	0.003	54.156	0.022
6	94.49	0.006	28.125	0.000	0.076	0.015	64.449
7	111.48	0.256	46.709	49.894	0.256	0.610	1.841
8	113.11	0.082	49.132	52.544	0.432	0.711	1.498
9	114.24	0.082	8.592	0.000	16.756	0.011	5.703
10	114.65	33.338	0.041	0.770	0.069	6.488	0.042
11	123.26	0.005	4.015	0.000	0.550	0.000	4.159
12	128.01	0.345	0.000	0.003	0.064	0.004	0.001
13	128.66	7.134	0.592	7.741	0.000	0.130	0.022
14	138.10	19.973	0.001	1.335	0.005	0.341	0.001
15	142.86	0.010	0.014	0.013	0.019	0.017	0.002
16	145.25	0.001	0.281	0.003	0.133	0.002	0.004
17	145.31	0.051	15.402	0.005	0.091	0.012	4.063
18	146.67	0.022	0.007	0.029	0.002	0.011	0.003
19	147.42	0.080	0.001	0.042	0.001	0.000	0.007
Static		336.063	336.063	336.063	48.414	343.560	331.745
residual		162.156	42.449	41.478	23.260	18.111	16.500

Table 5.4. *Effective mass model of Figure 3.11*

k	Mk	tk/|tk|			OG		(t.r)/(t.t)
1	92.80	0.0003	-1.0000	-0.0067	0.668	-0.001	0.242	-0.0035
2	47.90	0.0036	0.9999	-0.0124	2.002	-0.005	0.163	-0.0056
3	183.88	-0.1022	0.0003	-0.9948	1.188	-0.003	-0.122	0.0044
4	103.61	-0.9999	0.0074	0.0097	-0.001	0.004	-0.075	0.0018
5	7.24	-0.9840	0.0328	-0.1753	-0.478	0.058	2.692	-0.0785
6	28.13	0.0144	0.9999	-0.0005	1.513	-0.022	-0.052	0.0230
7	96.86	0.0514	-0.6944	-0.7177	-0.153	0.030	-0.040	-0.0465
8	101.76	-0.0284	-0.6949	0.7186	-0.144	-0.043	-0.048	0.0310
9	8.67	0.0973	0.9953	-0.0010	0.807	-0.080	-1.380	0.1703
10	34.15	0.9881	-0.0347	-0.1502	0.067	0.041	0.429	-0.0543
11	4.02	0.0335	0.9994	-0.0024	1.017	-0.035	-0.369	0.0209
12	0.35	0.9960	-0.0278	0.0852	0.007	-0.089	-0.117	-0.4185
13	15.47	-0.6792	-0.1956	-0.7074	-0.057	-0.022	0.061	0.0486
14	21.31	-0.9681	-0.0063	-0.2503	0.032	-0.003	-0.123	0.0161
15	0.04	-0.5213	0.6156	-0.5910	0.518	-0.312	-0.782	-0.0779
16	0.28	-0.0542	0.9934	-0.1007	0.112	-0.062	-0.675	-0.1322
17	15.46	-0.0573	-0.9982	0.0184	0.512	-0.031	-0.075	0.0232
18	0.06	-0.6105	0.3503	-0.7103	0.229	-0.279	-0.335	0.1856
19	0.12	0.8068	0.0707	0.5866	0.013	0.152	-0.037	-0.1998
r1	165.68	0.9859	-0.0084	-0.1673	0.004	0.001	0.021	-0.0012
r2	40.50	-0.0256	-0.9953	-0.0937	0.376	0.003	-0.130	0.0011
r3	36.46	0.1725	-0.0973	0.9802	0.314	-0.004	-0.056	0.0026
r4	0.67	0.0030	1.0000	0.0002	-0.685	0.001	5.748	-0.1084
r5	1.48	-0.1002	-0.0861	-0.9912	-3.089	0.003	0.312	0.0983
r6	1.29	0.0052	0.9995	-0.0319	-2.852	-0.002	-0.517	-0.0767

Table 5.5. *Ingredients of the effective mass model of Figure 3.11*

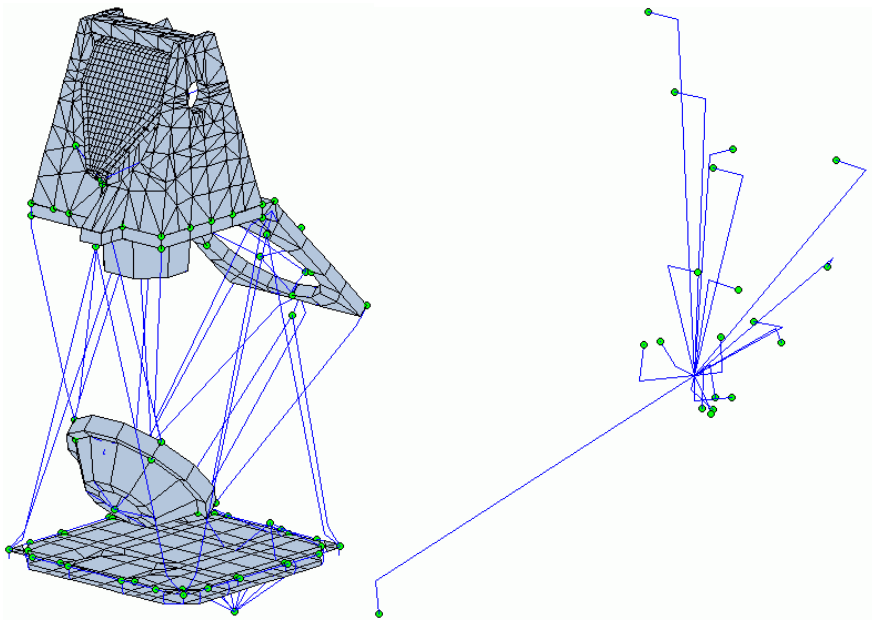

Figure 5.14. *Effective mass model of Figure 3.11*